Structural and elastic behavior of $Fe_{50}Al_{50}$ nanocrystalline alloys

E. Bonetti[a)] and G. Scipione
*Dipartimento di Fisica and Istituto Nazionale per la Fisica della Materia, Università di Bologna,
via Irnerio 46, I-40126 Bologna, Italy*

R. Frattini
*Dipartimento di Chimica Fisica and Istituto Nazionale per la Fisica della Materia, Università di Venezia,
D.D. 2137, I-30123 Venezia, Italy*

S. Enzo and L. Schiffini
*Dipartimento di Chimica and Istituto Nazionale per la Fisica della Materia, Università di Sassari,
via Vienna 2, I-07100 Sassari, Italy*

Pure iron and aluminum powders were mixed in the equiatomic ratio and mechanically alloyed in a high-energy ball mill for different times. Structure refinement of x-ray powder diffraction data was performed to study the structural transformations induced by mechanical and subsequent thermal annealing treatments. The mechanical alloying (MA) process induces a progressive dissolution of aluminum phase into the bcc iron phase. After 32 h of MA a single-phase Fe(Al) bcc extended solid solution, with lattice parameter $a_0 = 2.891$ Å, average coherent domain size $\langle D \rangle \approx 50$ Å, and lattice strain 0.5%, was observed. The annealing of the specimens after MA up to 8 h favored the aluminum dissolution in α-iron and the precipitation of the Al_5Fe_2 phase, whereas a nanostructured B2 FeAl intermetallic compound was observed in the annealed samples which were previously milled for 8, 16, and 32 h. In the same specimens a minority cubic phase Fe_3AlC_X, anti-isomorphous with perovskite, derived from contamination of ethanol and introduced in the steel vial as a lubricant agent, was also observed. Anelasticity measurements have shown the occurrence of two main transient effects during the first thermal run. The first one occurring at 500 K in all mechanically alloyed specimens was attributed to thermally activated structural transformations, whereas the second at about 700 K was attributed to a magnetic order–disorder transition. During the second run of anelasticity measurements a relaxation peak P_1 in the nanostructured B2 FeAl intermetallic compound, attributed to grain-boundary sliding mechanisms and with an activation energy of 1.8 ± 0.2 eV was observed. In specimens milled for 8–32 h a second small peak P_2 at the low-temperature tail of the P_1 peak was observed and tentatively attributed to a Zener-type relaxation. © *1996 American Institute of Physics.* [S0021-8979(96)01010-9]

I. INTRODUCTION

The mechanical properties of metals and compounds depend to a large extent on the grain size and on the nature and structure of the interfaces.[1] In many pure metals and alloys the reduction of grain size in the nanometer range is associated with an overall strength increase.[2] Further, the reported strong enhancement of diffusivity observed in nanophase materials,[3,4] attributed to grain-boundary mechanisms, should have relevant consequences on the ductility at relatively low temperatures.

In the intermetallic aluminides, particularly in the $Fe_{50}Al_{50}$ compound, one of the main drawbacks concerning their possible technological applications is the low ductility at room temperature and the poor strength at high temperatures.[5]

Two main approaches were generally followed to improve the ductility: The first consists in a careful control of grain-boundary cohesion by microalloying and the second in the improvement of the suitable grain refinement processing, such as inoculation, rapid solidification, and mechanical alloying (MA) techniques.[6] Some interdisciplinary studies on

iron aluminides, covering the general areas of processing (including MA), were recently reported.[7] The MA technique is receiving particular attention, as it appears suitable for the production of nanophase materials on industrial scale. Researches on the effects of the influence of strong mechanical working on Fe–Al alloys can be traced back to a early work by Taylor and Jones.[8] However, only recently Shingu *et al.*[9] reported the formation of nanocrystalline Fe–Al extended solid solutions by MA. Other studies deal with the Fe–Al system processed by MA or mechanical milling (MM) at different concentrations and particularly those corresponding to the stoichiometric compositions Fe_3Al and FeAl.[10–16] Kuhrt *et al.*[17] synthesized the $Fe_{50}Al_{50}$ composition in different MA conditions and established that moderate milling treatments are required to obtain a microstructural refinement and disordering. In previous articles we studied the micromechanisms of the solid-state reaction induced by the MA of the $Fe_{75}Al_{25}$ alloy as a function of milling conditions[18–21] and it was shown that a control of the milling procedures, combined with thermal aging after the cold consolidation of the milled powders, allows one to synthesize iron aluminides with grain size in the nanometer range. In the present work we have studied as a function of MA treatment the structural behavior and the thermal and mechanical stability of iron and

---
[a)]Electronic mail: bonetti@gpxbof.df.unibo.it

aluminum powders mixed in the equiatomic composition. In particular, we have focused our attention on the mechanisms of formation of a solid solution obtained after long time of MA, to the diffusivity of Al in the Fe(Al) solid solution, and to the interface mobility in the FeAl intermetallic. The experimental techniques employed for the characterization are x-ray diffraction (XRD), differential scanning calorimetry (DSC), and measurements of the elastic energy dissipation Q^{-1} and of the dynamic elasticity modulus M (mechanical spectroscopy).

II. EXPERIMENT

A. Synthesis of the Fe$_{50}$Al$_{50}$ alloy

Pure Fe and Al powders (44 μ, ALFA products, 99.9% purity) were milled in the equiatomic composition in a hardened tool steel vial of a SPEX mixer/mill model 8000 for 2, 4, 8, 16, and 32 h at room temperature. The weight of the mixed powders was about 10 g each time and the ball-to-powder weight ratio was 3:1. To minimize oxygen contamination the milling treatments were performed under argon atmosphere (oxygen <5 ppm). To avoid the sticking of aluminum to the walls of the vial during the process ethanol as a lubricant agent was added in the concentration of 0.05 ml/g of powder.

The consolidation procedure consisted in cold pressing 0.2 g of milled powder in a constructed die with a rectangular section 15×5 mm^2 by means of a piston under an axial pressure of about 1.5–2 GPa. In this way thin bar specimens with a thickness of 0.8 mm have been obtained.

B. Characterization techniques

XRD measurements were performed with a Bragg–Brentano goniometer, using Cu $K\alpha$ radiation ($\lambda=1.5418$ Å) and a monochromator in the diffracted beam. The data were analyzed with the Rietveld code FULLPROF, available from Rodriguez-Carvajal at the ILL Laboratory of Grenoble (France). This program is a structural refinement based on the calculation of the structure factor of the phases in the specimen. For each phase the intensity contribution is given by

$$I_{hkl}(q) = C m L_p \exp\left(\frac{-\sigma^2 q^2}{2}\right)$$
$$\times \left| \sum_j o_j f_j(q_{hkl}) \exp[2\pi i(hx_j+ky_j+lz_j)] \right|^2,$$
(1)

where hkl are the Miller indices defining the atomic planes, C is a scaling factor, m is the multiplicity factor, L_p is the Lorentz polarization factor, $\exp(-\sigma^2 q^2/2)$ is a Debye–Waller-like temperature factor, o_j is the site occupancy, f_j is the scattering factor of the jth atomic species, $q_{hkl}=(4\pi/\lambda)\sin\theta_{hkl}$ is the wave vector, θ_{hkl} is the Bragg angle, and x_j, y_j, and z_j are fractional atomic coordinates in the unit cell. Each I_{hkl} value was convoluted with pseudo-Voigt functions in order to account for the Bragg peak broadening due to instrumental factors and crystallite size
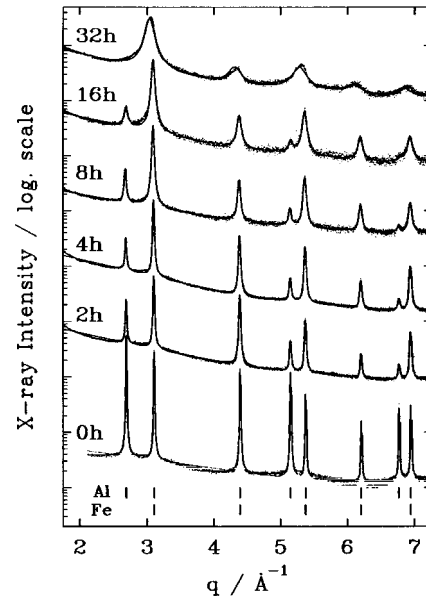

FIG. 1. XRD intensity (log scale) vs wave-vector q plot for the Fe$_{50}$Al$_{50}$ elemental powders milled at the times quoted. The aluminum peaks decrease slowly and disappear at 32 h of milling time. Dots are experimental data points and the solid line is the best-fitting curve of the Rietveld procedure.

reduction plus lattice disorder. The refined structural parameters were essentially the unit cell constant a_0 and the σ term. From the peak shape parameters, calculated with adjustable pseudo-Voigt functions,[22] we have calculated the integral peak breadth β_{hkl}. If β_{hkl} is plotted versus the wave vector q_{hkl} the slope of the trend is proportional to the average root-mean-squared strain $\langle\epsilon^2\rangle^{1/2}$ and the intercept to $q_{000}=0$ is inversely related to the average crystallite size $\langle D\rangle$.[23] DSC analyses were carried out with a DSC7 Perkin–Elmer calorimeter. The powders were crimped in aluminum pans and heated at a constant rate of 20 K/min under flow of purified argon. Measurements of the Young's modulus and elastic energy dissipation coefficient (internal friction) were performed on cold consolidated reed specimens in the range 0.1–30 Hz by an inverted torsion pendulum at a strain amplitude of about 10^{-4}. All measurements in isochronal conditions were performed at a constant heating rate of 2.5 K/min.

III. RESULTS AND DISCUSSION

A. Transient effects and structural evolution during MA

Figure 1 shows the XRD patterns of the Fe$_{50}$Al$_{50}$ powders (dotted lines) milled for the times quoted. The pattern of parent powder (bottom) displays narrow peak profiles due to bcc α-Fe and to fcc Al. It must be noted that the peaks of bcc iron are overlapped by the peaks of Al with the indices hkl all even, so that only the Al peaks with indices all odd are free from overlapping. To describe the structural evolution, we have carried out a whole-powder-pattern fitting analysis with the Rietveld method. The results are shown in Fig. 1 as solid lines. During the MA process the intensity of the non-overlapping peaks of Al decreases slowly with respect to that

Bonetti *et al.*

TABLE I. Phase analyses (molar percentage) performed with the Rietveld method for the as-milled powders and for the products after internal friction measurements.

Milling time (h)	After MA		After thermal aging				
	% bcc Fe	% Al	% Fe	% Al	% Al$_3$Fe$_2$	% FeAl	% Fe$_3$AlC$_x$
0	48	52	50	50	⋯	⋯	⋯
2	76	24	70	12	18	⋯	⋯
4	85	15	67	3	22	8	⋯
8	92	8	60		20	18	2
16	96	4	⋯		⋯	97	3
32	100	0	⋯		⋯	95	5

of the others, vanishing in the pattern of the alloy milled 32 h, where just the broad peaks of a bcc phase (solid solution) are evaluated. A quantitative analysis of the phases was carried out based on the best-fit values of the scaling factor C of each crystallographic phase and the results are reported in Table I, left-hand side. The scaling factors C are highly correlated to the Debye–Waller factors σ_j, so the data in Table I have an uncertainty of 15%. The data in Table II indicate an expansion of the lattice parameter of the bcc solid solution phase from $a_0 = 2.866$ Å (value for α-Fe) to $a_0 = 2.891$ Å. The modification of the lattice parameter is very small at short milling times whereas a significant change occurs between 16 and 32 h (Table II). This result is in agreement with the data reported by Hume-Rothery, Smallman, and Haworth[24] for Fe–Al alloys with Al concentration in the range 30–50 at. % prepared by slow-quenching methods. The work by Taylor and Jones[8] on Fe–Al bulk alloys produced by cold working gave similar results. Perez Alcazar and Galvão da Silva[25] reported larger values of the lattice parameter for the nearly equiatomic Fe–Al bcc phase prepared by quenching in ice (>2.92 Å). In addition, larger values of the lattice parameter were also reported by Sumyiama, Hirose, and Nakamura[26] in the case of Fe–Al equiatomic alloys obtained by vapor quenching.

The patterns of Fig. 1 show an increase of the peak broadening as a function of MA time, related to a reduction of the average crystallite size and/or to an increased level of strain. The values of the average crystallite size $\langle D \rangle$ and the average root-mean-squared strain $\langle \epsilon^2 \rangle^{1/2}$, calculated according to the integral breadth method of Wagner and Aqua[27] with an uncertainty of 10%, can be reasonably ascribed to the bcc phase and are reported in Table II, together with the values of $\langle D \rangle$ calculated from Al(111) peaks. Similar results

were obtained in the work reported by Oleszak and Shingu at short times of milling for a similar composition produced by a conventional horizontal low-energy ball mill.[16]

The MA treatment initially reduces the average crystallite size and increases the atomic strain level, with a limited dissolution of Al into the bcc lattice of α-Fe, as is testified by the presence of the Fe(Al) solid solution only for long milling times. This process seems complete in the specimen milled 32 h. This behavior is very similar to that observed for the Fe$_{75}$Al$_{25}$ composition,[18] but in the present case the process of dissolution is taking longer times of MA. This is attributed to the presence of ethanol used as lubricant to prevent the sticking of aluminum on the wall of the vial, as reported in Ref. 20.

The DSC traces of the mechanically alloyed samples are reported in Fig. 2 and show complex exothermic events in the temperature range 550–850 K, which consists of two different peaks for the specimens milled up to 16 h. In addition, the specimens milled 4 and 16 h were annealed at intermediate temperatures of 718 and 663 K, respectively, and
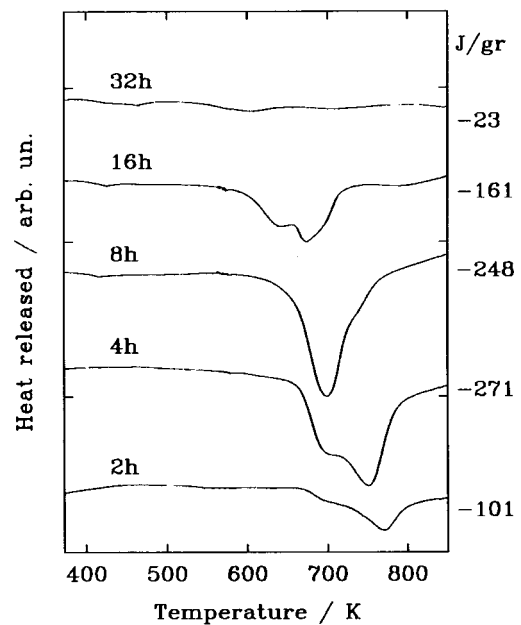
TABLE II. The refined structural parameters a_0 of the bcc solid solution phase, the average crystalline size $\langle D \rangle$, and $\langle D \rangle_{Al(111)}$, the average root-mean-squared strain $\langle \epsilon^2 \rangle^{1/2}$, and the variation of internal friction background ΔQ^{-1} for Fe$_{50}$Al$_{50}$ samples as a function of milling time.

Milling time (h)	2	4	8	16	32
$(a_0 \pm 0.001)$ Å	2.866	2.868	2.868	2.871	2.891
$\langle D \rangle$ (Å)	360	320	220	160	50
$\langle \epsilon^2 \rangle^{1/2} \times 10^{-3}$	0.57	0.87	1.4	2.5	6.2
$\langle D \rangle_{Al(111)}$ (Å)	240	190	160	105	
$(\Delta Q^{-1} \pm 0.02) \times 10^{-3}$					
400 K	6.31	5.21	2.11	1.19	0.0
500 K	4.80	3.15	1.28	1.01	0.0

FIG. 2. DSC traces of the Fe$_{50}$Al$_{50}$ samples at the scanning rate of 20 K/min for samples milled for the times indicated. Numbers on the right-hand side refer to the total heat released per gram (between room temperature and 900 K) for each sample.
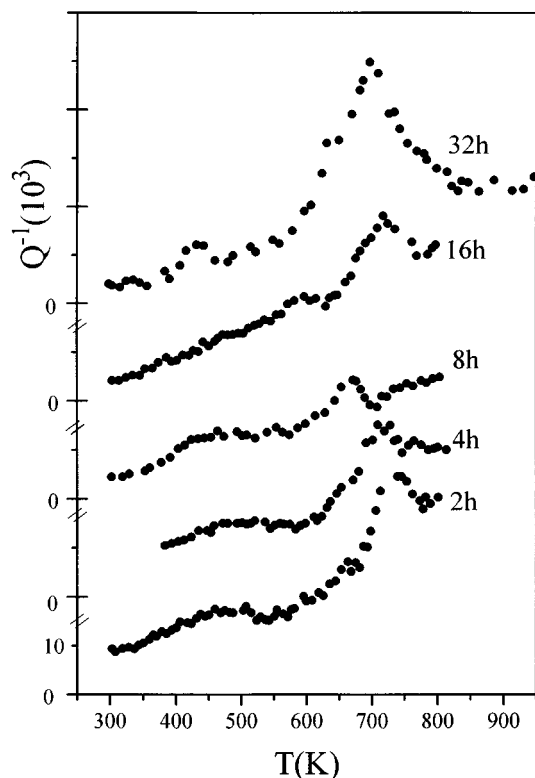
J. Appl. Phys., Vol. 79, No. 10, 15 May 1996

Bonetti et al.   7539

FIG. 3. Internal friction vs temperature of cold consolidated powders as a function of milling time. Frequency at 300 K ~2–3 Hz.

FIG. 4. Average crystalline size $\langle D \rangle$ vs temperature of the sample milled 32 h. The values of $\langle D \rangle$ at 663 and 873 K have been obtained submitting the sample at a constant heating rate of 20 K/min under flow of purified argon. The highest value refers to a vacuum anneal at 1223 K for 12 h.

examined with XRD to assess the structural transformations involved in the heat evolution. As reported in Ref. 28, it was found that the peak at 718 K of the alloy milled 4 h is related to the appearance of the Al_5Fe_2 phase, while for the sample milled 16 h the peak at 663 K is related to the occurrence of an Fe(Al) bcc solid solution. The heat evolution is the largest in the alloy milled 4 h (−271 J/g), while it is negligible in the specimen milled 32 h (−23 J/g).

The internal friction versus temperature trends during the first run on specimens mechanically alloyed at different times are reported in Fig. 3. A comparison with the curves obtained during the second run (Fig. 7) suggests that transient effects, due to the structural transformations thermally induced on the metastable phases achieved at different milling stages, mask the intrinsically anelastic relaxation effects occurring in a thermally stabilized condition. Main features in the damping spectra reported in Fig. 3 are the two damping maxima occurring at about 500 and 700 K. The first one is connected to a thermally activated structural relaxation, as evidenced by its disappearance after the first thermal run (see Fig. 7). A similar behavior was previously observed also on the $Fe_{75}Al_{25}$ compound.[18,19]

An indication of the amount of structural relaxation may be provided by the variation of the internal friction ΔQ^{-1}, measured in the temperature range of the maximum, i.e., in the 400–550 K range, of specimens milled for increasing times, with respect to that of the specimen milled 32 h, where the lowest values for the background damping are experienced. The small peak occurring in some samples milled for 32 h at 450 K and not observed during the second
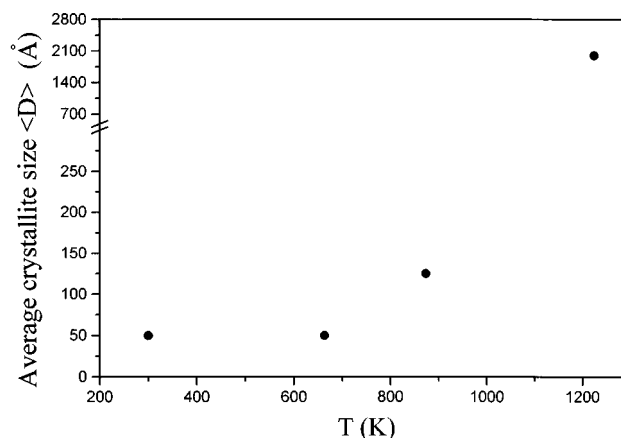
thermal run (Fig. 7) can be attributed to an anelastic relaxation produced by stress-induced ordering of interstitial impurities such as C in the bcc Fe(Al) solid solution.[29]

As shown in Table II ΔQ^{-1} reduces strongly for milling times in excess of 4 h. This strong reduction of internal friction background proceeds in parallel with the grain refinement (Table II). It is worth recalling that the average crystallite size corrected for disorder from the x-ray data of Table II contains also the contribution due to dislocations. According to early observations on several pure metals and alloys obtained by mechanical attrition and MA,[30,31] in the early milling stages a strong increase of the density of dislocations arranged in thick arrays inside grains occurs. Correspondingly an enhancement of the background damping may be expected. At higher milling times grain fragmentation and refinement occur up to an ultimate value, the dislocation density strongly decreases and thereafter also the background damping. This feature of the damping spectra was recently observed also on nanostructured metals.[32]

The second damping maximum at 700 K was attributed to a magnetic order–disorder transition, whose Curie temperature was found to decrease as a function of the Al content.[33] We have shown in Fig. 4 the average crystalline size $\langle D \rangle$ versus temperature of the sample milled 32 h obtained by XRD measurements. As can be seen, a significant grain growth starts above 700 K.

B. Stable phases and anelastic relaxation peaks

The dynamic Young's modulus curves of all specimens during the first thermal run display an increasing trend[34] in the range 500–800 K, where the internal friction maxima were observed (Fig. 3). On the contrary, after a first thermal run of anelasticity measurements up to 900 K, a monotonic decreasing trend has been observed (Fig. 5) with no significant differences with the successive thermal runs, suggesting that a relatively stable structural state is reached.

We have verified that the thermal stabilization brought about by the anelasticity measurements (two thermal runs up to 900 K) precipitated different phases depending on the pre-
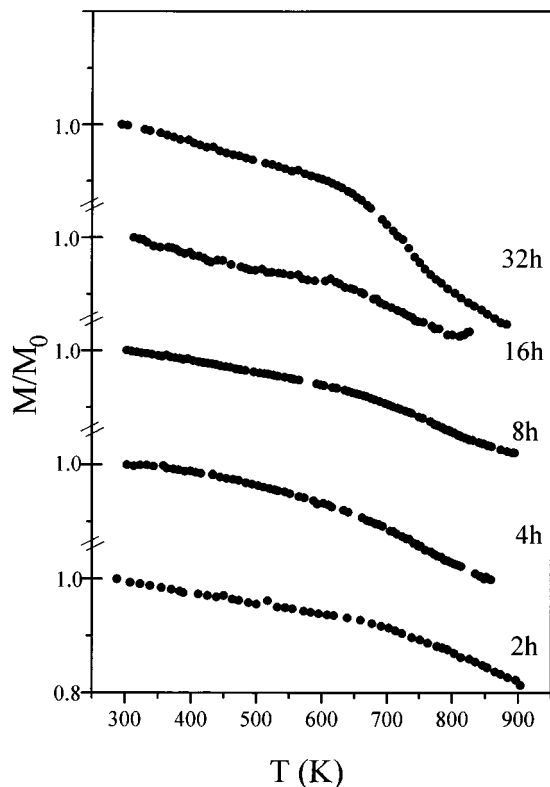
FIG. 5. Dynamic Young's modulus (M/M_0) vs temperature for cold consolidated powders as a function of milling time during the second measurement run. Frequency at 300 K ~3–5 Hz. M_0 is the room-temperature dynamic modulus value.

FIG. 7. Internal friction (Q^{-1}) vs temperature for the samples as in Fig. 3 during the second run. Frequency at 300 K ~3–5 Hz.

vious MA treatment, as shown by the XRD patterns of Fig. 6 (data points). The solid lines are the best-fit results obtained with the Rietveld method. The phase analysis reported in Table I, right-hand side, indicates that the specimen milled
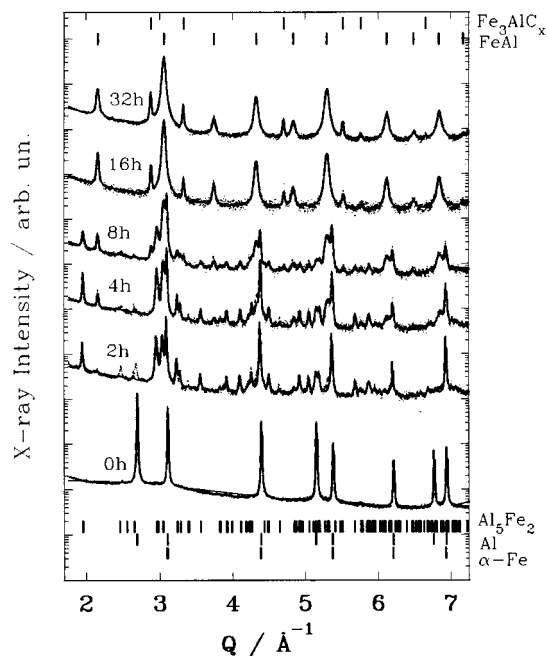

FIG. 6. XRD intensity (log scale) vs wave vector q plot for the $Fe_{50}Al_{50}$ elemental powders as in Fig. 1 after an internal friction up to 900 K.
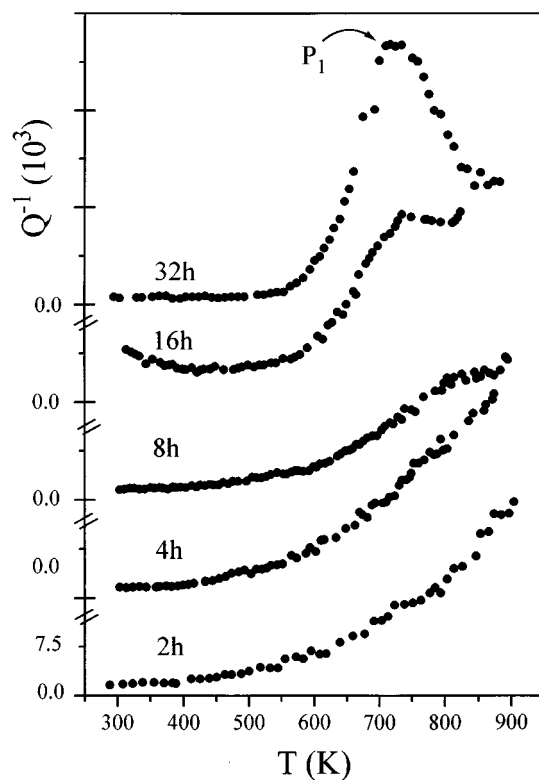
for 2 h precipitates first the Al_5Fe_2 intermetallic compound. After 4 h also the FeAl intermetallic starts to appear, followed, in the alloy milled 8 h, by the Fe_3AlC_x carbide. Note also in Table I that the specimens which were milled for 16 and 32 h decompose. After the internal friction run, only the FeAl (partially) ordered and the Fe_3AlC_x compounds are present. The molar percentages of these phases, calculated according to the method of Rietveld, are also given in Table I. The presence of the carbide phase can be related again to the use of ethanol in the vial. This observation was firstly established by Nasu et al.[35] after a Mössbauer study of Ag–Fe alloys produced by MA.

Figure 7 shows the internal friction versus temperature trends of the milled specimens during the second run. All curves display a background damping Q_B^{-1} increasing with temperature, that can be fitted according to the equation[36]

$$Q_B^{-1} = A_1 + A_2 \exp(-B/k_B T), \qquad (2)$$

where A_1 is a constant factor, k_B is the Boltzmann's constant, $A_2 = \omega^{-n}$, ω is the vibration frequency, $B = nH$, and H is an average activation energy. The values of n, determined by Q^{-1} measurements at different frequencies ω_i and calculated from a $\log(Q^{-1})$ $\log \omega$ plot, are reported in Table III for specimens milled at different hours. The expression (2) was originally proposed to fit the background damping at high temperatures in pure metals and alloys on the hypothesis of dissipative mechanisms due to dislocations and involving a not too wide spectrum of activation energies.[36] It can be noted (Table III) that the background activation energy H increases with the milling time above approximately 570 K.

TABLE III. Fitting of the background internal friction for $Fe_{50}Al_{50}$ samples milled for 4 and 32 h with the expression (see Ref. 36) $Q_B^{-1} = A_1 + A_2 \exp(-B/k_BT)$, where A_1 is a constant factor, $A_2 = \omega^{-n}$, $B = nH$, and H is an average activation energy.

Milling time (h)	T (K)	B (eV)	n	$H \pm 0.2$ (eV)
4	600	0.22	0.24	0.9
4	790	0.22	0.18	1.2
32	600	0.34	0.15	2.2
32	790	0.34	0.17	2.0

The results agree with the reported increase of the activation energy for self-diffusion in Fe–Al alloys on increasing the aluminum content.[37]

In Fig. 7 it is possible to observe with increasing milling time the growth of an internal friction peak P_1 of relaxational nature, whose relaxation strength strongly increases in the specimen milled 32 h. The peak temperature is correspondingly shifted to lower values as a function of the grain sizes. From the peak temperature shift as a function of the measuring frequency ω_i an activation energy can be evaluated from the expression[38]

$$H_1 = k_B \ln(\omega_2/\omega_1)\Delta(1/T)^{-1}, \qquad (3)$$

with $\Delta(1/T)^{-1} = (1/T_1 - 1/T_2)^{-1}$; T_i is the peak temperature corresponding to frequency ω_i.

Due to the limited frequency range investigated, the evaluation of H_1 is subjected to a rather high error as it can be judged from Fig. 8, from the extrapolated straight line an activation energy $H_1 = 1.8 \pm 0.2$ eV can be obtained. Consequently with this value we obtain from the Arrhenius equation $\tau = \tau_0 \exp(H/k_BT)$ a pre-exponential factor $\tau_0 = 10^{-14}$ s.

Note that the activation energy H_1 is definitely lower than that reported for creep in B2 ordered iron aluminides (3–4 eV).[39] This is not a surprising result as, in the case of pure metals with average grain size in the range of nanometers, high values of the diffusion coefficient were reported, attributed to an enhanced diffusion at the grain boundaries.[4,40] Furthermore, anelasticity measurements in nanostructured aluminum, prepared as thin film or in form of powders, seem to indicate that the activation energy for
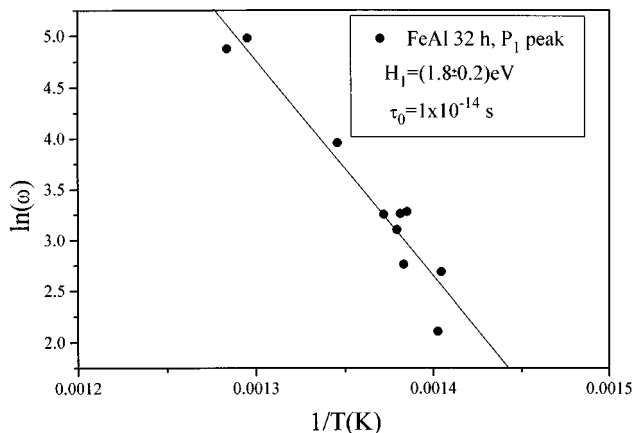

FIG. 8. Arrhenius plot (ln ω vs reciprocal temperature) for $Fe_{50}Al_{50}$ samples milled for 32 h.
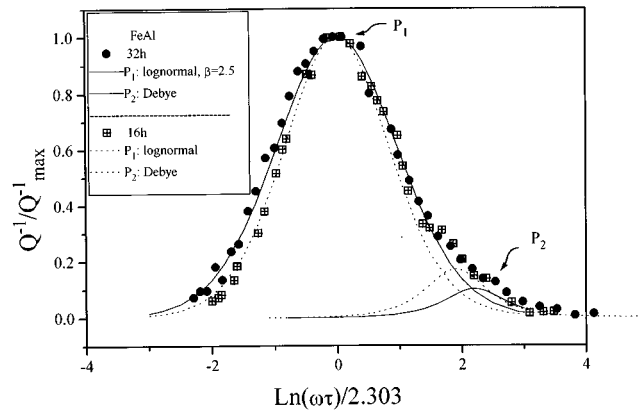

FIG. 9. Normalized internal friction (Q^{-1}/Q_{max}^{-1}) vs $\ln(\omega\tau)/2.303$ for samples milled for 16 h (centered box) and 32 h (solid circle). In both cases, the main peak (P_1) was fitted with a log-normal distribution function $\Phi(z)$ [Eq. (4)], while the P_2 peak was fitted with a Debye function (solid line and dots for the samples milled 32 and 16 h, respectively).

grain-boundary sliding is significantly lower than in coarse-grained materials.[41,42] A correlation between the activation energy and the formation of the carbide phase should be rejected, as the internal friction peak was also observed in specimens prepared without ethanol. In addition, a contribution from carbon segregation to the boundary is expected to enhance the peak energy, which is in contrast with the low activation energy found. After background removal from the curve of the specimen milled 32 h, a peak shape analysis was carried out by fitting the experimental data with a log-normal distribution of relaxation times (Fig. 9), according to the expression

$$\Phi(z) = \beta^{-1}\pi^{-1/2}\exp[-(z/\beta)^2], \qquad (4)$$

where β is a measure of the width of the distribution, $z = \ln(\tau/\tau_m)$, and τ_m is the mean relaxation time. Consequently, the expression of the elastic energy dissipation coefficient Q^{-1} for a Debye peak is modified as follows:[38]

$$Q^{-1} \cong \Delta_M \int_{-\infty}^{+\infty} \Phi(\ln \tau) \frac{\omega\tau}{1+(\omega\tau)^2} d(\ln \tau), \qquad (5)$$

where Δ_M is the relaxation strength.

The fitting procedure gives a value of $\beta = 2.5$, which may be probably accounted for a wide distribution of grain sizes. This hypothesis is supported by the super-Lorentzian shape of XRD line profiles in the specimens milled for long times.[43,44] The XRD patterns have shown that when a well-resolved P_1 peak occurs in the internal friction spectra (32 h), a homogeneous FeAl B2 nanophase, partially ordered, is formed. In the specimens milled 8, 16, and 32 h a careful analysis of the internal friction data reveals a peak asymmetry in the low-temperature tail that can be related to the presence of a second small peak P_2 (see Fig. 9). The attribution of this peak to a specific mechanism and a reliable evaluation of its activation energy becomes very questionable. It should be noted that a similar peak was recently observed in a nano-
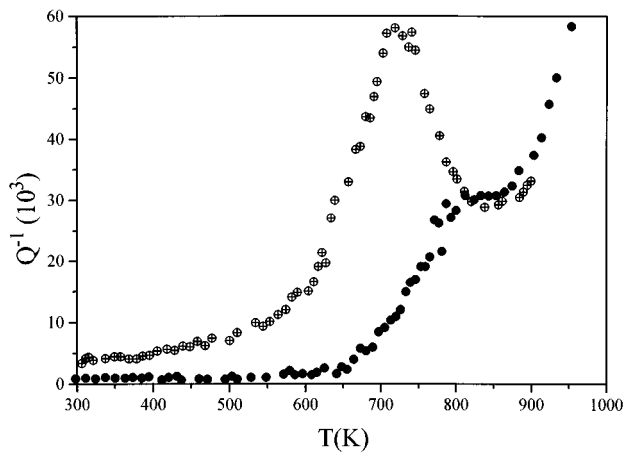
FIG. 10. Internal friction (Q^{-1}) vs temperature for samples respectively treated for 32 h of milling time and after the first heating run (centered circle) and after a successive aging treatment in vacuum at 1223 K for 12 h (solid circles).

structured $Fe_{75}Al_{25}$ milled alloy and was attributed to a Zener-type relaxation in the Fe(Al) solid solution.[21,45] In addition, in coarse-grained Fe–Al compounds Shyne and Sinnott[46] and Fishbach[47] reported that the strength for Zener-type relaxation reaches a maximum at an Al content of 20 at. % and then decreases for higher values. Strictly speaking, in a fully ordered FeAl compound the Zener relaxation should be absent, so the presence of the P_2 peak can be justified by the incomplete ordering of the FeAl phase, pointed out by the Rietveld fit of XRD patterns (long-range-order parameter of 0.80), and the heterogeneity of aluminum diffusion during the MA stages.[48] More systematic measurements, at present in progress, are necessary to clarify this point.

In coarse-grained Fe–Al compound, Hren[49] observed a peak at 1000 K, at a frequency of 1000 Hz, which was attributed to grain-boundary sliding. In an attempt to see whether our P_1 peak corresponds to that of Hren, we have submitted the specimens milled 32 h to a vacuum anneal at 1223 K for 12 h, after which the average grain size was increased up to 2000 Å (see Fig. 4). In Fig. 10, the peak temperature of the samples so treated appears to be clearly shifted 80–90 K and the peak height considerably reduced with respect to the unannealed specimen. On account of the frequency used by us (~4 Hz), compared to that of Hren's measurements (1000 Hz) and considering the H_1 value, it can be seen that at the highest frequency the P_1 peak temperature roughly corresponds to that observed by Hren. This may suggest that the relaxation mechanism is strongly dependent on the grain size and/or on the structure of the interfaces. However, in our case the influence of extrinsic features, such as segregated impurities (carbides), cannot be totally disregarded.

IV. CONCLUSIONS

The MA of pure iron and aluminum powders mixed in the equiatomic ratio produces an extended solid solution with the bcc structure and a lattice parameter expansion from the value of 2.866 Å for pure iron to 2.891 Å. After a ther-

mal treatment up to 900 K, the solid solution transforms in a partially ordered, nanostructured FeAl intermetallic compound. The anelasticity measurements in cold consolidated alloys have shown a well-resolved internal friction peak, associated with anelastic relaxation in the nanostructured B2 FeAl intermetallic compound, whose peak parameters are significantly different with respect to those measured in coarse-grained FeAl intermetallic. The further occurrence in the anelasticity spectra of a small relaxation peak tentatively attributed to a Zener-type mechanism in the Fe(Al) solid solution suggests an incomplete degree of chemical order in the nanophase intermetallic and/or an heterogeneous extended solid solution with aluminum concentration fluctuation.

[1] R. W. Siegel and G. E. Fougere, in *Nanophase Materials*, edited by G. C. Hadjipanais and R. W. Siegel (Kluwer, Dordrecht, 1994), p. 233.

[2] G. W. Nieman, J. R. Weertman, and R. W. Siegel, J. Mater. Res. **6**, 1012 (1991).

[3] H. J. Holfler, R. S. Averback, H. Hahn, and H. Gleiter, J. Appl. Phys. **74**, 3832 (1993).

[4] S. Schumacher, R. Birringer, R. Strauss, and H. Gleiter, Acta Metall. **37**, 2485 (1989).

[5] C. G. McKamey, J. H. Devan, P. F. Tortorelli, and V. K. Sikka, J. Mater. Res. **6**, 1779 (1991).

[6] T. Haubold, R. Bohn, R. Birringer, and H. Gleiter, Mater. Sci. Eng. A **153**, 679 (1992).

[7] *Processing, Properties, and Application of Iron Aluminides*, edited by J. H. Schneibel and M. A. Crimp (TMS, Warrendale, 1994).

[8] A. Taylor and R. M. Jones, J. Phys. Chem. Solids **6**, 16 (1958).

[9] P. H. Shingu, B. Huang, J. Kuyama, K. N. Ishihara, and N. Nasu, in *New Materials by Mechanical Alloying Techniques*, edited by E. Artz and L. Schultz (DGM Informationsgesellschaft, 1989), p. 319.

[10] M. A. Morris and D. G. Morris, Mater. Sci. Forum **88-90**, 529 (1992).

[11] Y. D. Dong, W. H. Wang, L. Liu, K. Q. Xiao, S. H. Tong, and Y. Z. He, Mater. Sci. Eng. A **134**, 867 (1991).

[12] E. P. Yelsukov, E. V. Voronina, and V. A. Barinov, J. Mag. Magn. Mater. **115**, 271 (1992).

[13] G. H. Fair and J. V. Wood, Powder Metall. **36**, 123 (1993).

[14] T. Zàk, O. Schneiweiss, Z. Cochnar, and A. Buchal, Mater. Sci. Eng. A **141**, 73 (1991).

[15] E. C. Deanne and R. F. Cochrane, in *Processing, Properties, and Application of Iron Aluminides*, edited by J. H. Schneibel and M. A. Crimp (TMS, Warrendale, 1994), p. 59.

[16] D. Oleszak and P. H. Shingu, Mater. Sci. Eng. A **181/182**, 1217 (1994).

[17] C. Kuhrt, H. Schorpf, L. Schulz, and E. Artz, in *Proceedings of the 2nd International Conference on Structural Applications of Mechanical Alloying*, Vancouver, September Metals Park (ASM, OH, 1993), p. 269.

[18] E. Bonetti, G. Scipione, G. Valdrè, G. Cocco, R. Frattini, and P. P. Macrí, J. Appl. Phys. **74**, 2053 (1993).

[19] E. Bonetti, G. Scipione, G. Valdrè, S. Enzo, R. Frattini, and P. P. Macrí, J. Mater. Sci. **30**, 2220 (1995).

[20] R. Frattini, L. Schiffini, G. Scipione, E. Bonetti, and S. Enzo, in *Processing, Properties, and Application of Iron Aluminides*, edited by J. H. Schneibel and M. A. Crimp (TMS, Warrendale, 1994), p. 79.

[21] E. Bonetti, G. Scipione, S. Enzo, R. Frattini, and L. Schiffini, Nanostruct. Mater. **6**, 397 (1995).

[22] S. Enzo, S. Polizzi, and A. Benedetti, Z. Kristallogr. **170**, 275 (1985).

[23] S. Enzo, G. Fagherazzi, A. Benedetti, and S. Polizzi, J. Appl. Crystallogr. **21**, 536 (1988).

[24] W. Hume-Rothery, R. E. Smallman, and C. W. Haworth, *The Structure of*

J. Appl. Phys., Vol. 79, No. 10, 15 May 1996

Bonetti *et al.* 7543

Metals and Alloys (The Institute of Metals, London, 1969), p. 172.

[25] G. A. Perez Alcazar and E. Galvão da Silva, J. Phys. F **17**, 2323 (1987).

[26] K. Sumyiama, Y. Hirose, and Y. Nakamura, J. Phys. Soc. Jpn. **59**, 2963 (1990).

[27] C. N. J. Wagner and E. N. Aqua, in *Advances in X-Ray Analysis*, edited by W. M. Mueller, G. R. Mallett, and M. J. Fay (Plenum, New York, 1964), Vol. 7, p. 46.

[28] S. Enzo, R. Frattini, R. Gupta, P. P. Macrí, G. Principi, L. Schiffini, and G. Scipione, Mater. Sci. Forum **195**, 31 (1995).

[29] A. Nowick and B. Berry, *Anelastic Relaxation in Crystalline Solids* (Academic, New York, 1972), p. 236.

[30] H. J. Fecht, E. Hellstern, Z. Fu, and W. L. Johnson, Metall. Trans. A **21**, 2333 (1990).

[31] H. J. Fecht, Nanostruc. Mater. **1**, 125 (1992).

[32] E. Bonetti and G. Valdrè, Philos. Mag. B **68**, 967 (1993).

[33] M. Yamamoto and S. Taniguchi, Sci. Rep. RITU A **8**, 112 (1956).

[34] E. Bonetti and G. Scipione, Mater. Sci. Forum (to be published).

[35] S. Nasu, P. H. Shingu, K. N. Ishihara, and F. E. Fujita, Hyperf. Inter. **55**, 1043 (1990).

[36] G. Snoek, E. Bisogni, and I. Shyne, Acta Metall. **12**, 1466 (1964).

[37] K. Hirano and A. Hishinuma, Nippon Kinzoku Gakkaishi **32**, 516 (1968).

[38] Reference 29, p. 61.

[39] A. Lawley, J. A. Coll, and R. W. Cahn, Trans. Am. Inst. Met. Eng. **218**, 166 (1960).

[40] J. Horvàt, R. Birringer, and H. Gleiter, Solid State Commun. **62**, 319 (1987).

[41] M. Prieler, H. G. Bohn, W. Schilling, and H. Trinkaus, Mater. Res. Soc. Symp. Proc. **308**, 305 (1993).

[42] A. Al Sadi, E. Bonetti, P. Mattioli, and G. Valdrè, J. Alloys Comp. **211-212**, 489 (1994).

[43] R. Del Maschio, S. Dirè, G. Carturan, S. Enzo, and L. Battezzati, J. Mater. Res. **7**, 435 (1992).

[44] J. Plevert and D. Louer, J. Chim. Phys. **87**, 1427 (1990).

[45] Reference 35, p. 248.

[46] J. C. Shyne and M. J. Sinnott, Trans. Metal. Soc. AIME **218**, 861 (1960).

[47] D. B. Fischbach, Acta Metall. **10**, 319 (1962).

[48] H. J. Fecht, G. Han, Z. Fu, and W. Johnson, J. Appl. Phys. **67**, 1744 (1990).

[49] J. A. Hren, Phys. Status Solidi **3**, 1603 (1963).